ISSN 0030-400X, Optics and Spectroscopy, 2013, Vol. 115, No. 3, pp. 335–339. © Pleiades Publishing, Ltd., 2013.
Original Russian Text © O.G. Romanov, D.V. Gorbach, A.L. Tolstik, 2013, published in Optika i Spektroskopiya, 2013, Vol. 115, No. 3, pp. 383–388.

BASIC PROBLEMS OF OPTICS 2012

Transformation of Optical Vortices by Polarization Dynamic Holograms

O. G. Romanov, D. V. Gorbach, and A. L. Tolstik
Belarus State University, Minsk, 220030 Belarus
e-mail: romanov@bsu.by, tolstik@bsu.by
Received January 22, 2013

Abstract—Results of theoretical and experimental studies of regularities in the transformation of the topological and polarization structures of optical vortices by polarization dynamic holograms formed by pulse Gaussian and singular light beams in dye solutions are presented.

DOI: 10.1134/S0030400X13090191

INTRODUCTION

Recording static or dynamic holograms involves, as a rule, similarly polarized waves, when the spatially modulated interference field of the reference and signal waves leads to recording holographic gratings due to spatial modulation of optical parameters of the photosensitive medium (variation of the refractive index and/or absorption coefficient). During the polarization holographic recording, the reference and signal waves are polarized orthogonally to each other, the total intensity of these waves remains constant, and only the spatial modulation of the light polarization state takes place in correspondence with the phase difference of waves recording the hologram [1]. As this takes place, the spatial-variable state of total field polarization causes the appearance of spatial modulation of photoanisotropy and/or photogyrotropy in the medium [2–4]. The passage to the polarization recording of holograms permits one to control for diffracted radiation polarization, which can be used, e.g., in laser radiation correction systems with a complex polarization distribution over the wavefront [5], as well as to obtain information about the structure and anisotropic properties of the medium, which has promising applications in systems of polarization optical memory [6].

Polarization recording of dynamic holograms in solutions of complex organic compounds (dyes) is possible due to induced anisotropy of medium absorption. At the same time, the effect of absorption saturation leads to manifestation of nonlinearities of the fifth and higher orders determining the possibility to implement nonlinear holographic recording of multiwave processes [7–9]. Multiwave interactions on the basis of nonlinear dynamic holograms, in turn, permit one to implement online control for the structure of optical vortices; it becomes possible to transform their wavefront [10], topological structure [11], and carrier wave frequency [12].

This work presents a theoretical analysis of transformation processes in the topological and polarization structures of optical vortices in the recording and reading scheme of transmitting dynamic polarization holograms, as well as results of experimental studies of regularities in the transformation of singular beams in the implementation of polarization four-wave interaction (FWI).

THEORETICAL MODEL

Let us consider the problem of the action of high-intensity polarized laser radiation on a resonant medium with allowance for two energetic states (ground and excited states). We suppose that light beam **E** propagates along the z axis and is linearly polarized along the x axis. Proceeding from kinetic equations for populations of the ground (n_1) and excited (n_2) energy levels [13], one can obtain stationary distribution functions in a unit of solid angle Ω depending on radiation intensity I and angle θ between electric vector **E** and dipole moment of molecules **D**:

$$n_1(I,\Omega) = \frac{1}{8\pi}\frac{2+3\alpha I\cos^2\theta}{1+3\alpha I\cos^2\theta}, \quad (1)$$

$$n_2(I,\Omega) = \frac{1}{8\pi}\frac{3\alpha I\cos^2\theta}{1+3\alpha I\cos^2\theta}, \quad (2)$$

where the coefficient $\alpha = (B_{12}+B_{21})/vp_{21}$ determines the saturation intensity of the resonance transition ($I_{sat} = \alpha^{-1}$), $B_{12,21}$ are the Einstein coefficients for stimulated transitions, P_{21} is the total probability of spontaneous and nonradiative transitions, and $v = c/n_0$ is the speed of light in a medium with a refractive index n_0.

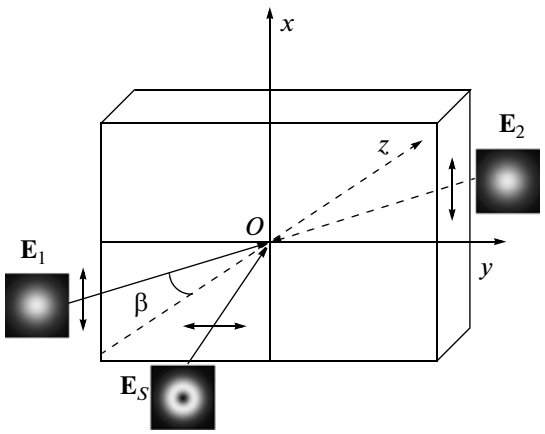

Fig. 1. Scheme of the formation of a 3D polarization hologram by a reference Gaussian and signal singular laser beams.

To describe the nonlinear response of an ensemble of two-level particles, we use the formalism of the complex refractive index $\hat{n} = n + i\kappa$. The extinction coefficients of the medium along the polarization axis x and axis y perpendicular to it are defined by the following expressions:

$$\kappa^{(x,y)} = \int \kappa^{(x,y)}(\Omega) d\Omega = \iint \kappa^{(x,y)}(\theta,\phi)\sin\theta d\theta d\phi, \quad (3)$$

where the functions

$$\kappa^{(x,y)}(\theta,\phi) = (\hbar c N/2v)(n_1 - n_2) b^{(x,y)}(\theta,\phi)$$

define the contribution of particles oriented in unit solid angle Ω to the extinction coefficient. Here, the differential Einstein coefficients for stimulated transitions are used:

$$b^{(x)}(\theta,\phi) = 3B\sin^2\theta\cos^2\phi,$$

$$b^{(y)}(\theta,\phi) = 3B\sin^2\theta\sin^2\phi,$$

$B_{12} = B_{21} \equiv B$ for the coinciding absorption and luminescence circuits. Integrating (3) over all angles θ and ϕ, we obtain the following expressions for the extinction coefficients of the medium along the polarization axis x and axis y perpendicular to it:

$$\kappa^{(x)} = 3\kappa_0\left[\frac{1}{3\alpha I} - \frac{\arctan\sqrt{3\alpha I}}{(3\alpha I)^{3/2}}\right], \quad (4)$$

$$\kappa^{(y)} = \frac{3}{2}\kappa_0\left[-\frac{1}{3\alpha I} + \left(\frac{1}{\sqrt{3\alpha I}} + \frac{1}{(3\alpha I)^{3/2}}\right)\arctan\sqrt{3\alpha I}\right], \quad (5)$$

where κ_0 is the (linear) extinction coefficient not depending on the intensity.

Let us calculate the anisotropy of the extinction coefficient $(\kappa_x - \kappa_y)/\kappa_0$ at a small intensity of the light beam ($\alpha I \ll 1$) using the expansion $\arctan\sqrt{3\alpha I} \sim \sqrt{3\alpha I}(1 - \alpha I)$:

$$(\kappa_x - \kappa_y)/\kappa_0 = 3\alpha I/2. \quad (6)$$

Similarly, one can calculate the anisotropy of the refractive index of a two-level resonant medium under the action of an intense polarized radiation:

$$(n_x - n_y)/\kappa_0 = 3\Theta\alpha I/2B, \quad (7)$$

where the function $\Theta(\omega)$ is connected with the Einstein coefficient for stimulated transitions $B(\omega)$ by the Kramers–Kronig relation. Thus, if the intensity of a light beam is much less than the saturation intensity of the resonant transition, this model describes the effects of light-induced anisotropy of the absorption coefficient and refractive index in the cubic nonlinearity approximation.

The considered model of the interaction between high-intensity linearly polarized radiation and a nonlinear originally isotropic medium was applied to describing the process of transformation of the spatial and topological structures of vortex optical beams in the process of recording and reading polarization holograms. We suppose that frequency ω of light beams $\mathbf{E}_1$ and $\mathbf{E}_S$ recording the dynamic hologram, as well as of reading beam $\mathbf{E}_2$, is close to the center of the absorption band $S_0 - S_1$ of the dye solution. Reference beam $\mathbf{E}_1$ with a Gaussian intensity distribution in the transverse profile and signal singular light beam $\mathbf{E}_S$ intersect in the volume of the nonlinear medium at small angle β and reading Gaussian beam $\mathbf{E}_2$ propagates exactly towards the beam $\mathbf{E}_1$ (Fig. 1).

We restrict our consideration to the case of linear mutually orthogonal polarization of the reference and signal beams ($\mathbf{E}_1 \parallel \mathbf{x}$, $\mathbf{E}_S \parallel \mathbf{y}$); in addition, we assume that polarization of the beam reading the dynamic hologram coincides with polarization of the reference beam ($\mathbf{E}_2 \parallel \mathbf{E}_1$). In this case, the total field of light waves can be represented in the form

$$\mathbf{E} = \mathbf{E}_1 + \mathbf{E}_S = \frac{1}{2}\left[\mathbf{e}_1 E_{1x}\exp i(\mathbf{k}_1\mathbf{r} - \omega t + \varphi_1) + \mathbf{e}_2 E_{Sy}\exp i(\mathbf{k}_S\mathbf{r} - \omega t + \varphi_S) + \text{c.c.}\right], \quad (8)$$

where $\mathbf{e}_1$ and $\mathbf{e}_2$ are unit vectors along the x and y axes, respectively, and $\mathbf{k}_1$ and $\mathbf{k}_S$ are wave vectors of the reference and signal waves.

Let us transform expression (8) to the form

$$\mathbf{E} = \begin{bmatrix} E_x \\ E_y \\ E_z \end{bmatrix} = \begin{bmatrix} p_x\cos\omega t + q_x\sin\omega t \\ p_y\cos\omega t + q_y\sin\omega t \\ 0 \end{bmatrix}, \quad (9)$$

where

$$p_x = E_{1x}\cos(\mathbf{k}_1\mathbf{r} + \varphi_1), \quad q_x = E_{1x}\sin(\mathbf{k}_1\mathbf{r} + \varphi_1),$$
$$p_y = E_{Sy}\cos(\mathbf{k}_S\mathbf{r} + \varphi_S), \quad q_y = E_{Sy}\sin(\mathbf{k}_S\mathbf{r} + \varphi_S).$$

Here, we put $E_z \approx 0$, which is a justified approximation at small angles of light beam convergence $2\beta < 5°$ [3]. Using expressions (9), one can determine the polarization state of the total field at each point of the space in the region where light beams $\mathbf{E}_1$ and $\mathbf{E}_S$ are overlapped. For example, expressions for parameters of the polarization ellipse of the total field (squares of the major and minor semiaxes a^2 and b^2, as well as the inclination angle between the major semiaxis and *Ox* axis) in the *xOy* plane have the form [3]

$$a^2 = \frac{1}{2}(I_1 + I_S) + \frac{1}{2}\sqrt{(I_1 + I_S)^2 - 4I_1I_S\sin^2[(\mathbf{k}_1 - \mathbf{k}_S)\mathbf{r} + \varphi_1 - \varphi_S]}, \quad (10)$$

$$b^2 = \frac{1}{2}(I_1 + I_S) - \frac{1}{2}\sqrt{(I_1 + I_S)^2 - 4I_1I_S\sin^2[(\mathbf{k}_1 - \mathbf{k}_S)\mathbf{r} + \varphi_1 - \varphi_S]}, \quad (11)$$

$$\sin 2\gamma = \frac{2\sqrt{I_1I_S}\cos[(\mathbf{k}_1 - \mathbf{k}_S)\mathbf{r} + \varphi_1 - \varphi_S]}{a^2 - b^2}, \quad \cos 2\gamma = (I_1 - I_S)/(a^2 - b^2). \quad (12)$$

Let us consider spatial distributions of parameters of the polarization ellipse of the total light field. A beam with a plane wavefront and Gaussian intensity distribution is taken as a reference beam E_1 (Fig. 2a):

$$E_{1x}(z = 0, r, \varphi) = E_{10}\exp[-(r/\sqrt{2}r_{01})^2],$$

for a signal beam, we take vortex beam E_S with a phase dislocation of topological charge *m* (Figs. 2b and 2c):

$$E_{Sy}(z = 0, r, \varphi) = E_{S0}[r/r_0]^{|m|}\exp[-(r/\sqrt{2}r_{0S})^2 + im\varphi].$$

To provide efficient overlapping of beams in the medium volume, the halfwidth of the reference beam was chosen to be twice the halfwidth of the signal beam ($r_{01} = 2r_{0S}$). Figures 2d and 2e present the spatial distributions of the inclination azimuth γ ($\pi/2 \geq \gamma \geq -\pi/2$) and ratios of semiaxes ($\delta = \pm\arctan(b/a)$, $\pi/2 \geq \delta \geq -\pi/2$) of the polarization ellipse of the total light field at the medium boundary $z = 0$. They were calculated by formulas (10)–(12) and take all possible values from the minimum (black color) to the maximum (white color). It is seen that spatially periodic distributions of parameters of the polarization ellipse of the total light field are formed in the region of light-beam overlapping and the ellipticity grating is characterized by a doubled spatial frequency with respect to the grating of the azimuth of the inclination angle of the polarization ellipse. The presence of fork dislocations in polarization patterns, which is typical for intensity interferograms of singular light beams [10], is explained by the indefiniteness of the phase in the center of signal beam $\mathbf{E}_S$.

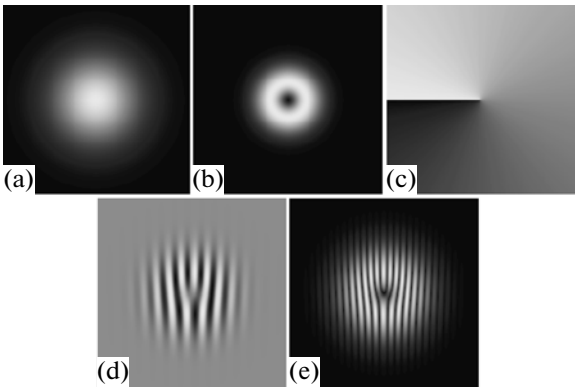

Fig. 2. Spatial profiles of the (a) reference and (b) signal light beams at the boundary $z = 0$, (c) signal beam wavefront, (d) distributions of the inclination azimuth and (e) ratios of semiaxes of the polarization ellipse of the dynamic grating.

Thus, analysis of the spatial-polarization distribution structure of the total field of the reference and signal beams permits one to conclude that polarization holograms containing information on the topological structure of optical vortices can be recorded in photoanisotropic media in the considered geometry.

For a counterpropagating reading wave,

$$\mathbf{E}_2 = (1/2)[\mathbf{e}_1E_{2x}\exp i(\mathbf{k}_2\mathbf{r} - \omega t + \varphi_2) + \text{c.c.}]$$

under the satisfied phase synchronism condition $\mathbf{k}_D = \mathbf{k}_1 - \mathbf{k}_S + \mathbf{k}_2$ in a cubically nonlinear medium, the polarization $\mathbf{P}_{\text{nl}} \sim \mathbf{e}_2\chi^{(3)}E_1E_2E_S^*$ is induced. In the low diffraction efficiency approximation with allowance for expressions (6) and (7) for the induced anisotropy, the equation for the complex amplitude of the diffracted wave $\mathbf{E}_D$ can be written in the form

$$\left(\frac{\partial}{\partial z} + \beta\frac{\partial}{\partial x} + \frac{\Delta_\perp}{2ik}\right)\mathbf{E}_D = -i\frac{k_0}{2}\mathbf{e}_2\frac{3}{8}\frac{\hat{\Theta}}{B}\alpha' E_1E_2E_S^*. \quad (13)$$

In this equation, $\Delta_\perp = \partial^2/\partial x^2 + \partial^2/\partial y^2$ is the transverse Laplacian, $k = \omega n_0/c$ is the wavenumber, k_0 is the linear absorption coefficient of the medium, $\hat{\Theta}(\omega) = \Theta(\omega) + iB(\omega)$ and $\alpha' = \alpha c n_0/8\pi$.

As follows from analysis of Eq. (13), diffracted wave $\mathbf{E}_D$ propagates precisely toward signal wave $\mathbf{E}_S$ and has the same polarization ($\mathbf{E}_D \parallel \mathbf{y}$). Moreover, using plane reference $\mathbf{E}_1$ and reading $\mathbf{E}_2$ waves ($\varphi_1 + \varphi_2 = \text{const}$) permits one to create a wavefront reversal effect at which the phase of diffracted wave $\mathbf{E}_D$ is formed reversely to the phase of signal wave $\mathbf{E}_S$ ($\varphi_D = -\varphi_S$). In the case in which signal beam $\mathbf{E}_S$ is characterized by the presence of topological charge *m*,

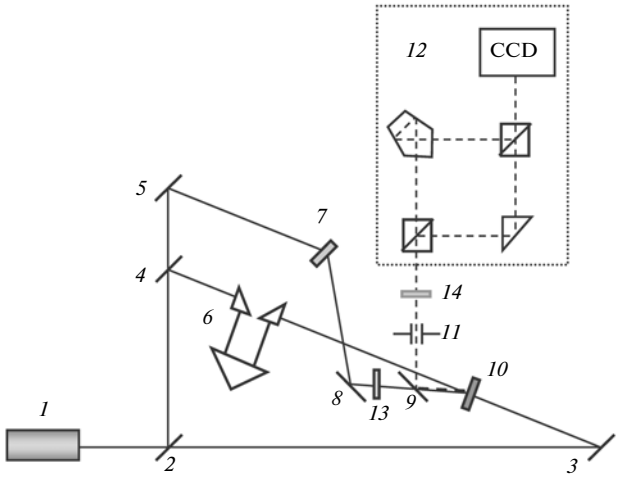

Fig. 3. Scheme of the experimental setup implementing the FWI of Gaussian and singular light beams.

reversed light beam $\mathbf{E}_D$ must contain a topological charge with the opposite sign $-m$.

EXPERIMENTAL RESULTS

Experimentally, the FWI of polarized Gaussian and singular light beams was studied during the record of transmitting dynamic holograms in the scheme of concurrent propagation of the reference and signal beams in a solution of the rhodamine 6Zh dye. The scheme of the experimental setup is presented in Fig. 3. YAG laser *1* (light beam divergence $\theta_{0.5} \le 2$ mrad and pulse duration $\tau = 20$ ns) operated in the mode of second radiation harmonic generation ($\lambda = 532$ nm). Reference $\mathbf{E}_1$ and signal $\mathbf{E}_S$ waves were formed by light-beam splitter *2* and mirrors *4* and *5*. To match the optical path length of the signal and reference waves, delay line *6* was used. The signal light beam with a screw dislocation of the wavefront was obtained using computer-synthesized transparencies *7* recorded in layers of polymethylmethacrylate with phenanthrenequinone [14]. The singular beam was directed to cell *10* with an ethanol solution of the 6Zh rhodamine dye at a small angle to the reference wave using mirror *8*. Reading wave $\mathbf{E}_2$ was directed to the cell with the dye solution precisely toward reference wave $\mathbf{E}_1$ using movable mirror *3*. The small angle ($2\beta \approx 30$ mrad) between the propagation directions of the reference and signal waves and transverse sizes of the beams ($r_{10} = 250$ μm and $r_{S0} = 75$–150 μm) provided an efficient spatial overlapping of the interacting light beams in the cell with the dye solution. The diffracted beam was segregated using semitransparent mirror *9* and diaphragm *11*. The spatial profiles of light-beam intensity were recorded using a CCD camera mounted at the output of Mach–Zehnder interferometer *12* permitting one to obtain interference patterns for the signal and diffracted light beams and identify their topological structure. Polarization of the interacting waves was varied by introducing half-wave phase plate *13* into the signal beam, and the polarization state of the reversed wave was analyzed using Glan prism *14*. The shape of the spatial distribution and topological structure of the reversed wave were also monitored in the course of the experiment. To record the spatial distribution of the beam, one of the arms of the Mach–Zehnder interferometer was overlapped and only one beam came to the camera.

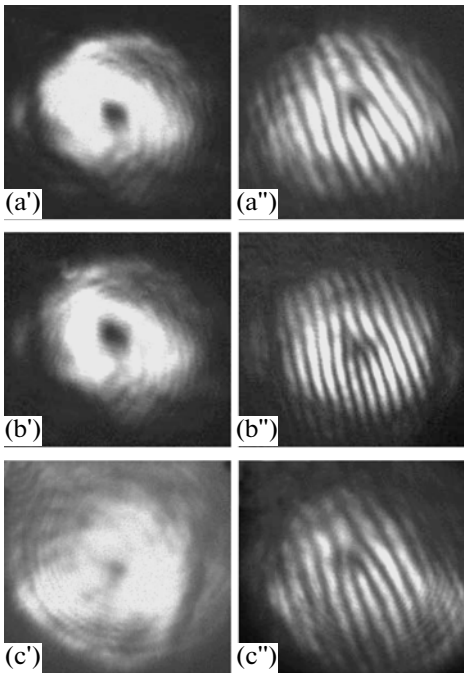

Fig. 4. Spatial profiles and interferograms (a) of the signal singular beam with topological charge $m = 1$ and diffracted beams at (b) similar and (c) orthogonal polarizations of the reference and signal beams.

Results of the experimental study of the FWI in an ethanol solution of the rhodamine 6Zh dye are shown in Fig. 4 presenting beam images obtained in the experiment (left column), as well as their corresponding interferograms (right column) verifying the presence of a topological charge.

At the initial stage, polarization of all the interacting waves was the same (vertical), which corresponded to the standard FWI scheme. The images in Figs. 4a' and 4a" correspond to signal beam $\mathbf{E}_S$. In this case, a singular beam with topological charge $m = 1$ was taken for the signal beam; this is verified by the interferogram in which, as follows from the form of the scheme used for detecting the charge, two interference fringes are added. Diffracted beam $\mathbf{E}_D$ (Figs. 4b' and 4b") was also vertically polarized and contained a topological charge equal to the signal beam charge in the absolute value. Note that the singular beam wavefront reversal that is implemented in standard FWI schemes leads to

changing of the sign of the topological charge [10]; however, to verify this fact, it is necessary to record interferograms of the signal and diffracted beams not with a plane wavefront, but with a spherical one [12].

Introducing phase plate $\lambda/2$ into the signal beam provided the implementation of the scheme of recording a polarization hologram by a reference Gaussian and signal singular light beams linearly polarized in mutually orthogonal planes, by analogy with the scheme presented in Fig. 1. The obtained images of diffracted beam $\mathbf{E}_D$ and the corresponding interferogram are presented in Figs. 4c' and 4c". Polarization of the diffracted beam coincided with that of the signal beam. Other possible combinations of orthogonal polarization of interacting waves were also obtained by placing a half-wave phase plate alternately to the reference and reading Gaussian light beams. Interferograms obtained in this way show that the topological charge introduced into the formed dynamic hologram is transferred to the reversed wave and is equal to the charge of signal wave $\mathbf{E}_S$ in the absolute value at any combination of polarizations of the interacting waves.

In conclusion, we note that the studied method of recording and reading polarization dynamic holograms in media with a photoinduced anisotropy of the absorptive and refractive indices opens additional possibilities for control for the structure of singular light beams, which can find applications, e.g., in implementing mathematical operations using the topological charge of optical vortices and their polarization state as logical items.

ACKNOWLEDGMENTS

The work was supported in part by the Belarusian Republic Foundation for Fundamental Research, project no. F11K-136.

REFERENCES

1. Sh. D. Kakichashvili, Opt. Spektrosk. **33**, 324 (1972).
2. T. D. Ebralidze, Appl. Opt. **34**, 1357 (1995).
3. T. Huang and K. H. Wagner, IEEE J. Quantum Electron. **31**, 372 (1995).
4. M. Xu, D. K. G. de Boer, C. M. van Heesch, A. J. H. Wachters, and H. P. Urbach, Opt. Express **18** (7), 6703 (2010).
5. V. I. Tarasashvili and A. L. Purtseladze, Opt. Spektrosk. **103** (6), 1046 (2007).
6. L. Nikolova and T. Todorov, J. Mod. Opt. **31**, 579 (1984).
7. A. Blouin and M. M. Denariez-Roberge, IEEE J. Quantum Electron. **29**, 227 (1993).
8. Diego J. L. Arce, Velez F. Fanjul, Cubian D. Pereda, A. L. Tolstik, O. G. Romanov, and O. Ormachea, Proc. SPIE—Int. Soc. Opt. Eng. **5710**, 159 (2005).
9. S. M. Karpuk, A. S. Rubanov, and A. L. Tolstik, Opt. Spektrosk. **80** (2), 313 (1996).
10. O. G. Romanov and A. L. Tolstik, Zh. Prikl. Spektrosk. **76** (3), 395 (2009).
11. O. G. Romanov and A. L. Tolstik, Opt. Spektrosk. **105** (5), 825 (2008).
12. O. G. Romanov, D. V. Gorbach, and A. L. Tolstik, Opt. Spektrosk. **108** (5), 812 (2010).
13. B. I. Stepanov and V. P. Gribkovskii, *Introduction into the Theory of Luminescence* (Izd. AN BSSR, Minsk, 1963) [in Russian].
14. U. V. Mahilny, D. N. Marmysh, A. L. Tolstik, V. Matusevich, and R. Kowarschik, J. Opt. A **10** (8), 085302 (2008).

Translated by A. Nikol'skii